PHYSICAL REVIEW A **109**, L021101 (2024)

Letter

Cm^{15+} and Bk^{16+} ion clocks with enhanced sensitivity to new physics

V. A. Dzuba and V. V. Flambaum
School of Physics, University of New South Wales, Sydney 2052, Australia

(Received 30 November 2023; accepted 10 January 2024; published 1 February 2024)

We perform calculations of the electronic structure of Cm^{15+} and Bk^{16+} ions and demonstrate that they have transitions which combine the features of atomic optical clocks with the enhanced sensitivity to the variations of the fine-structure constant α. The high sensitivity is due to large nuclear charge Z, high ionization degree Z_i, and the effect of *level crossing*, which enables optical transitions between states of different configurations. These are the $6p_{1/2}$-$5f_{5/2}$ and $6p_{1/2}$-$5f_{7/2}$ transitions in the single-valence electron approximation. The variation of α may be due to the interaction with scalar and pseudoscalar (axion) dark-matter fields. Therefore, Cm^{15+} and Bk^{16+} clocks are promising candidates to search for these fields.

DOI: 10.1103/PhysRevA.109.L021101

Presently the fractional precision of the frequency measurements in optical clock transitions of Sr, Yb, Al^+, Hg, Hg^+, and Yb^+ atomic systems has reached an unprecedented level of 10^{-18} (see, e.g., Refs. [1–7]). It is natural to use the advantage of so high accuracy of the measurements in search for the physics beyond the standard model, for example, search for the space-time variation of the fundamental constants such as the fine-structure constant α ($\alpha = e^2/\hbar c$). The variation of α may be due to the interaction of the electromagnetic field with scalar and pseudoscalar (axion) dark-matter fields [8–10]. Therefore, the measurement of α variation is one of the instruments to use in the search for dark matter.

The search for the slow drift of α can be performed by comparing the frequencies of atomic transitions with different sensitivities to the variation of α over a long period of time. The laboratory limits on the present-day time variation of α have already passed 10^{-18} per year (see, e.g., the measurements in Refs. [11–15] and review [16]).

The sensitivity of the atomic transitions to the variation of α used in these studies is not very high [17–19]. This is also true for all working atomic clocks. It was suggested in Ref. [20] to use optical transitions in highly charged ions (HCI) to achieve significantly stronger sensitivity to the α variation. Indeed, effects of α variation in electron energies are due to the relativistic corrections which increase proportional to $Z^2(Z_i+1)^2$ (Z_i is the ionization degree) [17,18,20]. Therefore, to have large effects we should consider heavy highly charged ions. To avoid cancellation between the relativistic shifts of upper and lower levels in an electronic transition we should consider transitions between different electronic configurations. However, frequencies of such transitions in HCI increase proportional to $(Z_i+1)^2$ and are usually far outside the laser range. The solution is based on the fact that ordering of the electron states depends on Z_i and by removing electrons we may achieve so-called *level crossing* bringing the frequencies of the transitions between states of different configurations into the optical region [21]. The biggest effects happen near the crossing between s and f, or $p_{1/2}$ and f, orbital energies [17,18,20,21]. The search for appropriate transitions in HCI is now a popular area of theoretical [22–30] and experimental [31–33] research (see also reviews [34,35]).

The highest sensitivity to α variation has been found in Cf^{17+} and Cf^{15+} ions [23,24,27,28]. These ions have all important factors of enhancement: high Z ($Z = 98$), high ionization degree, and optical transitions between states of different configurations which correspond to the $6p_{1/2}$-$5f$ transitions. The disadvantage of the use of Cf is its instability. The most long-lived isotopes of Cf are $^{249}\mathrm{Cf}$ (the half-life is 351 years) and $^{251}\mathrm{Cf}$ (the half-life is 898 years) [36]. Isotope $^{250}\mathrm{Cf}$ with zero nuclear spin lives only 13 years.

In the present work, we study the Cm^{15+} and Bk^{16+} ions. They are very similar to the Cf^{17+} ion in terms of electronic spectra and the sensitivity to the variation of α but have much longer-living isotopes. For example, the half-life of $^{247}\mathrm{Cm}$ is 15.6 million years, $^{248}\mathrm{Cm}$ with zero nuclear spin has a half-life of 0.348 million years, and the half-life of $^{247}\mathrm{Bk}$ is 1380 years [36]. In addition, the long-living isotopes of Cm and Bk have values of atomic number A lower than those of the long-living isotopes of Cf, which probably means that it is easier to produce them. The Cm^{15+}, Bk^{16+}, and Cf^{17+} ions share another important advantage—a relatively simple electronic structure. They have only one electron above closed subshells and only two states above the ground state in the optical region. This means that the high accuracy of the calculations is possible and interpretation of the experimental spectra may be relatively simple.

The energy diagram for the lowest states of Cm^{15+} and Bk^{16+} is presented in Fig. 1. It is based on the results of our calculations. We perform the calculations with the use of the combination of the configuration interaction (CI) with the single-double (SD) coupled-cluster methods [37,38]. The effects of various external fields (e.g., electromagnetic multipole fields for calculating transition amplitudes, hyperfine interaction, etc.) are included within the well-known random-phase approximation (RPA). The details of the calculations are presented in the Appendix. The results for the energy

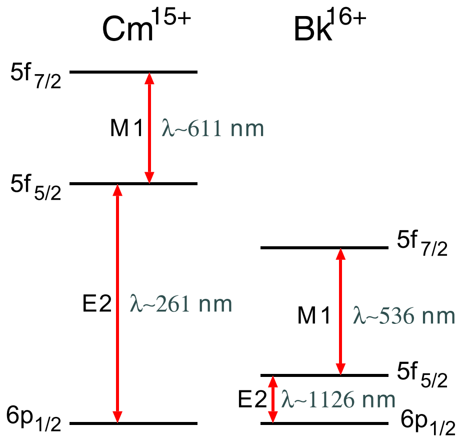

FIG. 1. Energy level diagram for the Cm^{15+} and Bk^{16+} ions (approximately in scale). Possible clock transitions are shown as red double arrows.

levels and other parameters for the lowest states of Cm^{15+} and Bk^{16+}, which are of odd parity, are presented in Table I. Similar parameters of Cf and Es ions obtained in earlier calculations [23,27] are presented in Table II for the convenience of comparison. The other states of the odd parity are at very high excitation energies, $E \sim 500\,000$ cm^{-1}.

Table III presents the lowest energy levels of even states. Electric dipole transitions from these states to $6s^2\,6p$ and $6s^2\,5f$ may, in principle, help to measure the frequencies of very weak clock transitions, which can be found as the difference of frequencies of E1 transitions from one of high even state to the $6s^2\,6p_{1/2}$ and $6s^2\,5f_{5/2}$ states. Moreover, the measurement of any energy interval between the states of $6s^2\,6p$ and $6s6p5f$ configurations may help to significantly improve the accuracy of the theoretical prediction of the small energy interval between the clock states. Indeed, this interval is much smaller than the removal energy of electrons. For example, the calculated ionization potential of Cm^{15+} is 2 168 971 cm^{-1}, which is 57 times bigger than the energy interval between the $5f_{5/2}$ and $6p_{1/2}$ states. This energy interval may be treated as the difference of removal energies of $5f_{5/2}$ and $6p_{1/2}$. Therefore, one may expect that the relative theoretical error for this energy interval is 50 times bigger than the relative error in the ionization potential. However, energy intervals within the same configuration (e.g., the fine splitting) have been calculated very accurately and reliably since there are no cancellations here. For example, if the energy of optical transition between $6s^2\,6p_{3/2}$ and any $6s6p5f$ states is measured, we may significantly reduce theoretical error in the energy interval between the $5f_{5/2}$ and $6p_{1/2}$ states.

TABLE I. Parameters of the lowest states of Cm^{15+} and Bk^{16+} ions: excitation energies (E), sensitivity coefficients (q), enhancement factors (K), lifetimes (τ), static dipole polarizabilities (α_0), electric quadrupole moments (Q), and magnetic dipole hyperfine-structure constants (A); $g_I = \mu/I$, where I is nuclear spin.

State	E (cm^{-1})	q (cm^{-1})	K	τ	α_0 (a_0^3)	Q ($\lvert e\rvert a_0^2$)	A/g_I (GHz)
				Cm^{15+}			
$6p_{1/2}$	0	0	0		1.1998	0	154
$5f_{5/2}$	38375	367000	15	576 ms	1.2460	−0.459	1.55
$5f_{7/2}$	54730	380000	13	20 ms	1.2433	−0.550	0.689
$6p_{3/2}$	182359						
				Bk^{16+}			
$6p_{1/2}$	0	0	0		1.0685	0	174
$5f_{5/2}$	8880	403000	91	787 s	1.1091	−0.507	1.74
$5f_{7/2}$	27520	419000	30	13 ms	1.1069	−0.604	0.772
$6p_{3/2}$	202403						

TABLE II. Transitions in Cf and Es ions sensitive to variation of α (from Refs. [23,27]). Notation J^p indicates total angular momentum of the state and its parity.

	Ground state		Clock state		E	q	
Ion	Conf.	J^p	Conf.	J^p	(cm^{-1})	(cm^{-1})	K
Cf^{15+}	$5f6p^2$	$5/2^-$	$5f^26p$	$9/2^-$	12314	380000	57[a]
Cf^{16+}	$5f6p$	3^+	$6p^2$	0^+	5267	−370928	−141[b]
Cf^{16+}	$5f6p$	3^+	$5f^2$	4^+	9711	414876	85[b]
Cf^{17+}	$5f$	$5/2^-$	$6p$	$1/2^-$	18686	−449750	−48[b]
Es^{16+}	$5f^26p$	$9/2^-$	$5f^26p$	$5/2^-$	6994	−184000	−53[a]
Es^{17+}	$5f^2$	4^+	$5f6p^3$	2^+	7445	−46600	−13[a]

[a] Ref. [27].

[b] Ref. [23].

To calculate the sensitivity of the atomic frequencies to the variation of α, we present them in the form

$$\omega(x) = \omega_0 + q\left[\left(\frac{\alpha}{\alpha_0}\right)^2 - 1\right] \equiv \omega_0 + qx, \tag{1}$$

where ω_0 and α_0 are present values for the frequency and the fine-structure constant, and q is the sensitivity coefficient. The values of q are found as a numerical derivative of the calculated values of the frequencies. It is also convenient to have the so-called enhancement factor K ($K = 2q/\omega$). It relates the rates of the changing frequencies and α. For the

TABLE III. Lowest even energy levels (cm^{-1}) of Cm^{15+} and Bk^{16+}.

Conf.	J Cm^{15+}	E	Conf.	J Bk^{16+}	E
$6s6p^2$	1/2	220159	$6s6p5f$	5/2	215399
$6s6p5f$	5/2	234517	$6s6p5f$	7/2	228430
$6s6p5f$	7/2	246936	$6s6p5f$	3/2	229257
$6s6p5f$	3/2	250537	$6s6p^2$	1/2	229273
$6s6p5f$	5/2	253281	$6s5f^2$	7/2	232137
$6s6p5f$	7/2	255862	$6s6p5f$	5/2	233227
$6s6p5f$	5/2	274931	$6s6p5f$	7/2	238672
$6s6p5f$	7/2	275226	$6s5f^2$	3/2	245731
$6s5f^2$	7/2	281399	$6s5f^2$	5/2	249308
$6s5f^2$	3/2	290189	$6s6p5f$	7/2	256126
$6s5f^2$	5/2	294383	$6s6p5f$	5/2	257240
$6s5f^2$	1/2	314906	$6s5f^2$	1/2	270551
$6s5f^2$	3/2	319212	$6s5f^2$	3/2	274819
$6s5f^2$	3/2	325976	$6s5f^2$	3/2	282097
$6s5f^2$	1/2	339563	$6s5f^2$	1/2	295155

relative variation of the ratio of the frequencies ω_1/ω_2, we have

$$\frac{\dot{\omega}_1}{\omega_1} - \frac{\dot{\omega}_2}{\omega_2} = (K_1 - K_2)\frac{\dot{\alpha}}{\alpha}. \tag{2}$$

The calculated values of q and K for the lowest states of Cm^{15+} and Bk^{16+} ions are presented in Table I. The values are given with respect to the ground state. These values indicate very high sensitivity of the ionic frequencies to the variation of α. The values of q and K are comparable to those for Cf and Es ions [23,27] (see Table II) and much bigger than the values of q and K in existing atomic clocks [19].

Note that all transitions in Table I are the $6p$-$5f$ transitions and corresponding values of q and K are positive. On the other hand, some transitions in Cf and Es ions are the $5f$-$6p$ transitions and corresponding values of q and K are negative (see Table II). This brings an opportunity for extra enhancement. For example, if the frequency of the transition in Bk^{16+} at $E = 8880\ \mathrm{cm}^{-1}$ is compared to the frequency of the transition in Cf^{16+} at $E = 5267\ \mathrm{cm}^{-1}$, then Eq. (2) becomes

$$\frac{\dot{\omega}_1}{\omega_1} - \frac{\dot{\omega}_2}{\omega_2} = 232\frac{\dot{\alpha}}{\alpha}. \tag{3}$$

This is the largest enhancement found in actinide ions so far.

Note, however, that larger values of q are more important than larger values of K. This is because the enhancement factor K can have a large value due to the small value of the transition frequency (like the $6p_{1/2}$-$5f_{5/2}$ transition in Bk^{16+}). Having a small value of the transition frequency does not always bring a significant advantage; see Ref. [39] for a detailed discussion.

The lifetimes of the $5f_{5/2}$ states of the Cm^{15+} and Bk^{16+} ions presented in Table I are determined by the electric quadrupole (E2) transition to the ground state. The lifetimes of the $5f_{7/2}$ states are strongly dominated by the magnetic dipole (M1) transition to the $5f_{5/2}$ states. See the Appendix for the calculation of the amplitudes. The $5f_{5/2}$ state of Bk^{16+} has a very long lifetime of ~800 s due to the small frequency of the transition to the ground state (transition rate $\propto \omega^5$). The lifetimes of other states in Table I are also relatively large. This means that high accuracy of the measurements is possible.

We consider now some sytematic effects in the frequency measurements.

Blackbody radiation (BBR) shift. The BBR shift of the transition frequency (in hertz) is given by (see, e.g., Ref. [40])

$$\delta\nu_{\mathrm{BBR}} = -8.611 \times 10^{-3}\left(\frac{T}{300\ K}\right)^4 \Delta\alpha_0. \tag{4}$$

Here $\Delta\alpha_0$ is the difference in the static scalar polarizabilities of two states (in a.u.). We calculate the polarizabilities as described in the Appendix. The results are presented in Table I. Using these numbers, at $T = 300$ K, we get the values for the relative frequency shift which are presented in Table IV.

TABLE IV. Relative frequency shift due to BBR in Cm^{15+} and Bk^{16+}.

Ion	Transition	$\delta\nu_{\mathrm{BBR}}/\nu$
Cm^{15+}	$6s_{1/2}$-$5f_{5/2}$	-3.4×10^{-19}
	$5f_{5/2}$-$5f_{7/2}$	2.2×10^{-20}
Bk^{16+}	$6s_{1/2}$-$5f_{5/2}$	-1.5×10^{-18}
	$5f_{5/2}$-$5f_{7/2}$	3.4×10^{-20}

Quadrupole shift. The $5f$ states have sufficiently large values of the total angular momentum J to make them sensitive to the gradient of electric field ε via quadrupole interaction. The corresponding energy shift is given by

$$\Delta E_Q = \frac{J_z^2 - J(J+1)}{2J(2J-1)} Q \frac{\partial \varepsilon_z}{\partial z}, \tag{5}$$

where Q is atomic quadrupole moment defined as the doubled expectation value of the E2 operator in the stretched state:

$$Q = 2\langle J, J_z = J|\mathrm{E2}|J, J_z = J\rangle. \tag{6}$$

The calculated values of the quadrupole moment Q for low states of Cm^{15+} and Bk^{16+} are presented in Table I. These values are close to those calculated for Cf^{15+} and Cf^{17+} in Ref. [28]. Therefore, the same estimate is valid: $\delta\nu/\nu \sim 10^{-16}$. These shifts can be further suppressed by up to 4 orders of magnitude by averaging over projections of the total angular momentum J [41].

Hyperfine structure. Hyperfine structure may complicate the work with the ions. In particular, it leads to enhancement of the second-order Zeeman shift, since small hyperfine intervals go into denominators of the expression for the shift. This complication can be easily avoided for Cm^{15+} ion. The isotope $^{248}\mathrm{Cm}$ lives 348 000 years and has zero nuclear spin. Bk has no long lifetime isotopes with zero nuclear spin since it has an odd number of protons. In any case, it is useful to know the values of the hyperfine constants for future analysis. We calculate the magnetic dipole constant A as described in the Appendix. The results are presented in Table I in the form of A/g_I ($g_I = \mu/I$, I is nuclear spin), which is approximately the same for all isotopes.

Sympathetic cooling. Ion-based optical clocks are susceptible to thermal motion due to the finite ion temperature. This motion can be reduced by applying sympathetic cooling of the clock ion via the cotrapped logic ion. The most efficient sympathetic cooling occurs when the charge-to-mass ratio of the clock ion is equal to that of the logic ion [42]. The Z_i/A ratio is 0.0605 for $^{248}\mathrm{Cm}^{15+}$ and 0.0648 for $^{247}\mathrm{Bk}^{16+}$. A possible logic ion in both cases is $^{24}\mathrm{Mg}^{+}$ where the Z_i/A ratio is 0.042.

In summary, we state that the Cm^{15+} and Bk^{16+} ions may serve as optical clocks which are not sensitive to external perturbations (BBR shift, quadrupole shift, etc.), but are very sensitive to the hypothetical time variation of the fine-structure constant and dark-matter fields.

Acknowledgment. This work was supported by the Australian Research Council under Grants No. DP230101058 and No. DP200100150.

Appendix: Method of calculations. We treat the Cm^{15+} and Bk^{16+} ions as systems with three valence electrons above the closed-shell $[1s^2 \dots 5d^{10}]$ core. Calculations start from the relativistic Hartree-Fock (RHF) procedure for the closed-shell core. The RHF Hamiltonian has the form

$$\hat{H}^{\mathrm{RHF}} = c\alpha \cdot \mathbf{p} + (\beta - 1)mc^2 + V_{\mathrm{nuc}} + V_{\mathrm{Breit}} + V_{\mathrm{QED}} + V_{\mathrm{core}}, \quad \text{(A1)}$$

where c is the speed of light, α and β are Dirac matrices, $\mathbf{p}$ is the electron momentum, V_{nuc} is the nuclear potential obtained by integrating the Fermi distribution of nuclear charge, V_{Breit} is the potential due to the Breit interaction [43], V_{QED} is the potential describing quantum electrodynamic corrections [44], and V_{core} is the self-consistent RHF potential created by all core electrons. The single-electron basis states for valence electrons are calculated in the field of the frozen core using the B-spline technique [45]. These basis states are used in all consequent calculations. This corresponds to the so-called V^{N-M} approximation [46], where M is the number of valence electrons ($M = 3$ in our case).

The SD coupled-cluster method is used (we use the version described in Ref. [38]) to include the correlations between valence and core electrons. Solving the SD equations involves iterations for the core and for the valence states until the full convergence is achieved. As a result, the all-order correlation operators $\hat{\Sigma}_1$ and $\hat{\Sigma}_2$ are produced. The $\hat{\Sigma}_1$ operator is the single-electron operator which describes the correlation interaction of a particular valence electron with the core. The $\hat{\Sigma}_2$ operator is the two-electron operator which describes the screening of the Coulomb interaction between valence electrons by the core electrons. The resulting effective CI Hamiltonian has the form

$$\hat{H}^{\mathrm{CI}} = \sum_{i=1}^{M} \left(\hat{H}^{\mathrm{RHF}} + \hat{\Sigma}_1\right)_i + \sum_{i<j}^{M} \left(\frac{e^2}{r_{ij}} + \hat{\Sigma}_{2ij}\right). \quad \text{(A2)}$$

The energy and the wave function of the many-electron state a are found by solving the CI equation

$$(\hat{H}^{\mathrm{CI}} - E_a)X_a = 0, \quad \text{(A3)}$$

where X_a contains coefficients of the expansion of the valence wave function over single-determinant basis states.

To calculate transition amplitudes or hyperfine structure we need to include an additional operator of the external field, such as magnetic dipole or electric quadrupole laser field, magnetic dipole nuclear field, etc. This is done within the RPA.

The RPA equations have the form (see, e.g., Ref. [47])

$$(\hat{H}^{\mathrm{RHF}} - \epsilon_c)\delta\psi_c = -(\hat{F} + \delta V_{\mathrm{core}})\psi_c, \quad \text{(A4)}$$

where $\hat{H}^{\mathrm{RHF}}$ is given by Eq. (A1), index c numerates single-electron states in the core, ψ_c and $\delta\psi_c$ are corresponding single-electron functions and corrections due to the operator of the external field $\hat{F}$, and δV_{core} is the change of the self-consistent Hartree-Fock potential due to the change in all core functions. Solving Eqs. (A4) self-consistently allows us to determine δV_{core}. Then the transition amplitude is given by

$$A_{ab} = \langle X_b | \sum_{i=1}^{M} (\hat{F} + \delta V_{\mathrm{core}})_i | X_a \rangle, \quad \text{(A5)}$$

where the wave functions for states a and b come from solving the CI equation (A3). For the energy shift (e.g., in calculating the hyperfine constant), $a = b$ in Eq. (A5).

Polarizabilities are calculated using the wave functions found as described above and the techniques of summations over the complete set of intermediate states as described in Refs. [48,49].

---

[1] I. Ushijima, M. Takamoto, M. Das, T. Ohkubo, and H. Katori, Cryogenic optical lattice clocks, Nat. Photon. **9**, 185 (2015).

[2] T. L. Nicholson, S. L. Campbell, R. B. Hutson, G. E. Marti, B. J. Bloom, R. L. McNally, W. Zhang, M. D. Barrett, M. S. Safronova, G. F. Strouse, W. L. Tew, and J. Ye, Systematic evaluation of an atomic clock at 2×10^{-18} total uncertainty, Nat. Commun. **6**, 6896 (2015).

[3] N. Huntemann, C. Sanner, B. Lipphardt, Chr. Tamm, and E. Peik, Single-ion atomic clock with 3×10^{-18} systematic uncertainty, Phys. Rev. Lett. **116**, 063001 (2016).

[4] A. D. Ludlow, W. F. McGrew, X. Zhang *et al.*, Optical frequency measurements at 1×10^{-18} uncertainty with ytterbium optical lattice clocks, *in Proceedings of Conference on Precision Electromagnetic Measurements (CPEM), Paris, France, July 8–13* (IEEE, Piscataway, NJ, 2018).

[5] W. McGrew, X. Zhang, R. Fasano, S. Schäffer, K. Beloy, D. Nicolodi, R. Brown, N. Hinkley, G. Milani, M. Schioppo *et al.*, Atomic clock performance enabling geodesy below the centimetre level, Nature (London) **564**, 87 (2018).

[6] S. M. Brewer, J.-S. Chen, A. M. Hankin, E. R. Clements, C. W. Chou, D. J. Wineland, D. B. Hume, and D. R. Leibrandt, $^{27}\mathrm{Al}^{+}$ Quantum-logic clock with a systematic uncertainty below 10^{-18}, Phys. Rev. Lett. **123**, 033201 (2019).

[7] T. Bothwell, C. Kennedy, A. Aeppli, D. Kedar, J. Robinson, E. Oelker, A. Staron, and J. Ye, Resolving the gravitational redshift across a millimetre-scale atomic sample, Nature (London) **602**, 420 (2022).

[8] A. Arvanitaki, J. Huang, and K. van Tilburg, Searching for dilaton dark matter with atomic clocks, Phys. Rev. D **91**, 015015 (2015).

[9] Y. V. Stadnik and V. V. Flambaum, Can dark matter induce cosmological evolution of the fundamental constants of Nature? Phys. Rev. Lett. **115**, 201301 (2015).

[10] Y. V. Stadnik and V. V. Flambaum, Improved limits on interactions of low-mass spin-0 dark matter from atomic clock spectroscopy, Phys. Rev. A **94**, 022111 (2016).

[11] T. Rosenband, D. B. Hume, P. O. Schmidt, C. W. Chou, A. Brusch, L. Lorini, W. H. Oskay, R. E. Drullinger, T. M. Fortier, J. E. Stalnaker, S. A. Diddams, W. C. Swann, N. R. Newbury, W. M. Itano, D. J. Wineland, and J. C. Bergquist, Frequency ratio of Al^{+} and Hg^{+} single-ion optical clocks, Science **319**, 1808 (2008).

[12] N. Leefer, C. T. M. Weber, A. Cingöz, J. R. Torgerson, and D. Budker, New limits on variation of the fine-structure constant using atomic dysprosium, Phys. Rev. Lett. **111**, 060801 (2013).

[13] R. M. Godun, P. B. R. Nisbet-Jones, J. M. Jones, S. A. King, L. A. M. Johnson, H. S. Margolis, K. Szymaniec, S. N. Lea, K. Bongs, and P. Gill, Frequency ratio of two optical clock transitions in $^{171}\mathrm{Yb}^{+}$ and constraints on the time variation of fundamental constants, Phys. Rev. Lett. **113**, 210801 (2014).

[14] M. Filzinger, S. Dörscher, R. Lange, J. Klose, M. Steinel, E. Benkler, E. Peik, C. Lisdat, and N. Huntemann, Improved limits on the coupling of ultralight bosonic dark matter to photons from optical atomic clock comparisons, Phys. Rev. Lett. **130**, 253001 (2023).

[15] N. Sherrill, A. O. Parsons, C. F. A. Baynham, W. Bowden, E. Anne Curtis, R. Hendricks, I. R. Hill, R. Hobson, H. S. Margolis, B. I. Robertson, M. Schioppo, K. Szymaniec, A. Tofful, J. Tunesi, R. M. Godun, and X. Calmet, Analysis of atomic-clock data to constrain variations of fundamental constants, New J. Phys. **25**, 093012 (2023).

[16] M. S. Safronova, D. Budker, D. DeMille, D. F. Jackson Kimball, A. Derevianko, and C. W. Clark, Search for new physics with atoms and molecules, Rev. Mod. Phys. **90**, 025008 (2018).

[17] V. A. Dzuba, V. V. Flambaum, and J. K. Webb, Space-time variation of physical constants and relativistic corrections in atoms, Phys. Rev. Lett. **82**, 888 (1999).

[18] V. A. Dzuba, V. V. Flambaum, and J. K. Webb, Calculations of the relativistic effects in many-electron atoms and space-time variation of fundamental constants, Phys. Rev. A **59**, 230 (1999).

[19] V. V. Flambaum and V. A. Dzuba, Search for variation of the fundamental constants in atomic, molecular and nuclear spectra, Can. J. Phys. **87**, 25 (2009).

[20] J. C. Berengut, V. A. Dzuba, and V. V. Flambaum, Enhanced laboratory sensitivity to variation of the fine-structure constant using highly charged ions, Phys. Rev. Lett. **105**, 120801 (2010).

[21] V. V. Flambaum and S. G. Porsev, Enhanced sensitivity to the fine-structure constant variation in Th IV atomic clock transition, Phys. Rev. A **80**, 064502 (2009).

[22] J. C. Berengut, V. A. Dzuba, V. V. Flambaum, and A. Ong, Hole transitions in multiply-charged ions for precision laser spectroscopy and searching for variations in α, Phys. Rev. Lett. **106**, 210802 (2011).

[23] J. C. Berengut, V. A. Dzuba, V. V. Flambaum, and A. Ong, Optical transitions in highly charged californium ions with high sensitivity to variation of the fine-structure constant, Phys. Rev. Lett. **109**, 070802 (2012).

[24] J. C. Berengut, V. A. Dzuba, V. V. Flambaum, and A. Ong, Highly charged ions with $E1$, $M1$, and $E2$ transitions within laser range, Phys. Rev. A **86**, 022517 (2012).

[25] V. A. Dzuba, A. Derevianko, and V. V. Flambaum, Ion clock and search for the variation of the fine structure constant using optical transitions in Nd^{13+} and Sm^{15+}, Phys. Rev. A **86**, 054502 (2012).

[26] V. A. Dzuba, V. V. Flambaum, and H. Katori, Optical clock sensitive to variation of the fine structure constant based on the Ho^{14+} ion, Phys. Rev. A **91**, 022119 (2015).

[27] V. A. Dzuba, M. S. Safronova, U. I. Safronova, and V. V. Flambaum, Actinide ions for testing the spatial α-variation hypothesis, Phys. Rev. A **92**, 060502(R) (2015).

[28] S. G. Porsev, U. I. Safronova, M. S. Safronova, P. O. Schmidt, A. I. Bondarev, M. G. Kozlov, I. I. Tupitsyn, and C. Cheung, Optical clocks based on the Cf^{15+} and Cf^{17+} ions, Phys. Rev. A **102**, 012802 (2020).

[29] C. Cheung, M. S. Safronova, S. G. Porsev, M. G. Kozlov, I. I. Tupitsyn, and A. I. Bondarev, Accurate prediction of clock transitions in a highly charged ion with complex electronic structure, Phys. Rev. Lett. **124**, 163001 (2020).

[30] V. A. Dzuba and V. V. Flambaum, The Os^{16+} and Ir^{17+} ions as candidates for accurate optical clock sensitive to physics beyond standard model, Phys. Rev. A **108**, 053111 (2023).

[31] H. Bekker, A. Borschevsky, Z. Harman, C. H. Keitel, T. Pfeifer, P. O. Schmidt, J. R. Crespo López-Urrutia, and J. C. Berengut, Detection of the $5p$-$4f$ orbital crossing and its optical clock transition in Pr^{9+}, Nat. Commun. **10**, 5651 (2019).

[32] T. Nakajima, K. Okada, M. Wada, V. A. Dzuba, M. S. Safronova, U. I. Safronova, N. Ohmae, H. Katori, and N. Nakamura, Visible spectra of highly charged holmium ions observed with a compact electron beam ion trap, Nucl. Instrum. Methods Phys. Res., Sect. B **408**, 118 (2017).

[33] A. Windberger, O. O. Versolato, H. Bekker, N. S. Oreshkina, J. C. Berengut, V. Bock, A. Borschevsky, V. A. Dzuba, Z. Harman, S. Kaul, U. I. Safronova, V. V. Flambaum, C. H. Keitel, P. O. Schmidt, J. Ullrich, and J. R. Crespo Lopez-Urrutia, Identification of optical transitions in complex highly charged ions for applications in metrology and tests of fundamental constants, Phys. Rev. Lett. **114**, 150801 (2015).

[34] M. G. Kozlov, M. S. Safronova, J. R. Crespo López-Urrutia, and P. O. Schmidt, Highly charged ions: Optical clocks and applications in fundamental physics, Rev. Mod. Phys. **90**, 045005 (2018).

[35] Y.-M. Yu, B. K. Sahoo, and B.-B. Suo, Highly charged ion (HCI) clocks: Frontier candidates for testing variation of fine-structure constant, Front. Phys. **11**, 1104848 (2023).

[36] J. K. Tuli, National Nuclear Data Center, www.nndc.bnl.gov.

[37] M. S. Safronova, M. G. Kozlov, W. R. Johnson, and D. Jiang, Development of a configuration-interaction plus all-order method for atomic calculations, Phys. Rev. A **80**, 012516 (2009).

[38] V. A. Dzuba, Combination of the single-double coupled cluster and the configuration interaction methods: Application to barium, lutetium and their ions, Phys. Rev. A **90**, 012517 (2014).

[39] V. A. Dzuba, V. V. Flambaum, and S. Schiller, Testing physics beyond the standard model through additional clock transitions in neutral ytterbium, Phys. Rev. A **98**, 022501 (2018).

[40] S. G. Porsev and A. Derevianko, Multipolar theory of blackbody radiation shift of atomic energy levels and its implications for optical lattice clocks, Phys. Rev. A **74**, 020502(R) (2006); Multipolar theory of blackbody radiation shift of atomic energy levels and its implications for optical lattice clocks, **86**, 029904(E) (2012).

[41] P. Dubé, A. A. Madej, Z. Zhou, and J. E. Bernard, Evaluation of systematic shifts of the ^{88}Sr^{+} single-ion optical frequency standard at the 10^{-17} level, Phys. Rev. A **87**, 023806 (2013).

[42] J. B. Wübbena, S. Amairi, O. Mandel, and P. O. Schmidt, Sympathetic cooling of mixed-species two-ion crystals for precision spectroscopy, Phys. Rev. A **85**, 043412 (2012).

[43] V. A. Dzuba, V. V. Flambaum, and M. S. Safronova, Breit interaction and parity non-conservation in many-electron atoms, Phys. Rev. A **73**, 022112 (2006).

[44] V. V. Flambaum and J. S. M. Ginges, Radiative potential and calculations of QED radiative corrections to energy levels and electromagnetic amplitudes in many-electron atoms, Phys. Rev. A **72**, 052115 (2005).

[45] W. R. Johnson and J. Sapirstein, Computation of second-order many-body corrections in relativistic atomic systems, Phys. Rev. Lett. **57**, 1126 (1986).

[46] V. A. Dzuba, V^{N-M} approximation for atomic calculations, Phys. Rev. A **71**, 032512 (2005).

[47] V. A. Dzuba, V. V. Flambaum, P. G. Silvestrov, and O. P. Sushkov, Correlation potential method for the calculation of energy levels, hyperfine structure and E1 transition amplitudes in atoms with one unpaired electron, J. Phys. B: At. Mol. Phys. **20**, 1399 (1987).

[48] V. A. Dzuba and A. Derevianko, Dynamic polarizabilities and related properties of clock states of the ytterbium atom, J. Phys. B **43**, 074011 (2010).

[49] V. A. Dzuba, Calculation of polarizabilities for atoms with open shells, Symmetry **12**, 1950 (2020).